

Albumin Binding and Anticancer Studies of trimethyl-, and triphenylstannyl (4R)-4-((3R,5R,10S,12S,13R,17R)-3,12-dihydroxy-10,13-dimethylhexadecahydro-1H-cyclopenta[a]phenanthren-17-yl)pentanoate

F. Shaheen^{1*}, S. Ali², T. Amir³, G. Wagnières⁴, V. Huntosova⁴

¹Department of Chemistry, Faculty of Science, Allama Iqbal Open University H-8/4 Campus Islamabad 44310, Pakistan

²Department of Chemistry, Faculty of Science, Quaid-i-Azam University, Islamabad 45320, Pakistan

³Department of Chemistry, Faculty of Basic Science, University of Wah, Quaid Avenue Wah, 47040, Pakistan

⁴Ecole polytechnique fédérale de Lausanne Institut des sciences et ingénierie chimiques
EPFL SB ISIC LCOM CH H5 595 (Bâtiment CH) Station 6 CH-1015 Lausanne Switzerland

Corresponding author: farzanaqau2103@gmail.com

Abstract

Trimethyl- (1) and triphenyl tin (2) derivatives of sodium (R)-4-[(3R,5R,8R,9S,10S,12S,13R,14S,17R)-3,12-dihydroxy-10,13-dimethyl-hexadecahydro-1H-cyclopenta[a]phenanthren-17-yl] pentanoate (sodium deoxycholate) were synthesized by refluxing sodium deoxycholate with the corresponding triorganotin(IV) chlorides in equimolar ratio. The two compounds were characterized by elemental analysis, infrared spectroscopy, ¹H, ¹³C, ¹¹⁹Sn NMR spectroscopy. Based on FT-IR spectra, $\Delta\nu$ values anticipated bridging or chelating behavior of the ligand. Both the compounds gave a trigonal bipyramidal geometry in the solid state and tetrahedral geometry in solution. The interaction of (1) and (2) with bovine and human serum albumin was investigated at two different temperatures (298 and 310K) utilizing fluorescence quenching experiments. Fluorescence quenching constants were determined from the Stern-Volmer equation. Both the compounds bind with Bovine serum albumin (BSA) and Human serum albumin (HAS) through a dynamic quenching pathway. Compound 1 binds with BSA and HSA at two temperatures with an association constant of 3.9×10^4 and 8.0×10^4 at 298K and 9.9×10^4 and 1.02×10^4 at 310K, respectively. Similarly, compound 2 binds with BSA and HSA with quenching constants of 3.9×10^4 and 1.8×10^4 at 298K and 1.4×10^4 and 4.5×10^4 respectively. The synchronous fluorescence spectrum of compounds suggested that the tryptophan residues contribute significantly to intrinsic fluorescence quenching.

Keywords: Fluorescence, Quenching, Bovine, Synchronous

1. INTRODUCTION:

Organometallic compounds have brought revolutionary advancement in all life sciences domains, and most of the compounds have acquired the rank of drug [1,2]. Among these, Organotin(IV) compounds, particularly the organotin(IV) carboxylates are interesting class of compounds which possess diverse structure types and applications in biological and nonbiological system [3, 4]. Understanding the pharmacodynamics and pharmacokinetics of these compounds/drugs in vivo requires their binding affinity and strength with biomolecules like DNA, albumin, etc. Among vertebrates, albumin is the most abundant protein (up to 40 mg/ml) and the most prominent plasma protein constituting about 60% of the total protein content of plasma [5]. It performs many functions, e.g., an organism's transport, distribution, metabolism, and excretion. Organotin(IV) complexes have been studied for a couple of years for their ability to interact and bind with various biomolecules like DNA [6], amino acids [7], flavonoids [8], proteins, enzymes [9], and carbohydrates [10]. Jing Sun et al., [9] studied the interaction of organotin(IV) compounds with HSA by using capillary electrophoresis coupled with inductively coupled plasma mass spectrometry [11]. So far, there are no comprehensive reports available in the literature on the interactions and the kinetics of organotin compounds with Human serum albumin (HSA) and Bovine serum albumin (BSA) by using fluorescence spectroscopy. The interaction of organotin (IV) compounds with HSA is essential to get an insight into the mechanism of organotin compounds' transportation and biological function in human bodies. Though various organometallic complexes are subjected to serum protein interaction studies, there is no report in the literature concerning the serum albumin protein interaction for organotin (IV) complexes by fluorescence spectroscopy. There is a great need to draw attention in this direction to get a deep insight into mechanistic aspects. BSA and HSA were selected for this purpose. Various techniques can be used to study protein interaction studies. Fluorescence quenching is a valuable and new technique used for protein interaction analyses. Sodium deoxycholate is common bile salt which aids in emulsification and solubilization of poorly soluble drugs.

In view of the above finding, and to explore the possible fate of the organotin(IV) compounds in body. The synthesized compounds were subjected to Bovine and Human serum albumins interaction studies.

2. EXPERIMENTAL:

2.1. Materials and Methods:

Bovine serum albumin (BSA) and Human serum albumin (HSA) were purchased from Sigma Aldrich. Both HSA and BSA were dissolved independently in phosphate saline buffer at pH = 7.4 to obtain final concentration of 10 μ M each. Similarly

4 different concentrations of 1.66 μM , 3.34 μM , 4.99 μM , and 6.64 μM were prepared separately for trimethyl and triphenylstannyl(4R)-4-[(3R,5R,10S,12S,13R,17R)-3,12-dihydroxy-10,13-dimethylhexadecahydro-1H-cyclopenta[a]phenanthren-17-yl] pentanoate. The fluorescence quenching measurements of BSA and HSA were carried out in Perkin Elmer LS 50B luminescence spectrometer equipped with 1 cm quartz cells and a thermostatic bath (Varian Cary Peltier System) at two temperatures (298 and 310 K). Initially, BSA and HSA were run in the absence of compounds, and then the effect was monitored by increasing concentrations. The excitation wavelength was 280 nm and the emission was monitored at a 300-500 nm range. The width of both excitation and emission slits was set at 5 nm. Spectra of phosphate buffer solutions, run under the same conditions, were taken as blanks and subtracted from the sample spectra.

The absorption spectra were measured on Cary 500 UV-Vis spectrophotometer in the range 250-800 nm. The concentrations of BSA and HSA were kept constant while varying the concentration of triorgonotin(IV) carboxylate complexes.

Synchronous fluorescence spectra were recorded at two different temperatures (298 and 310 K), in the absence and presence of varying complex concentrations for BSA. The excitation wavelength was 250-320 nm and the emission was monitored at 330 nm. The width of both excitation and emission slits was set at 5 nm. Spectra were recorded at $\Delta\lambda = 15$ and 60 nm.

2.2. Synthesis of complex (1) and (2)

The compounds were synthesized and well characterized by the method reported by our group [10]. Trimethyl- (1) and triphenyl tin (2) derivatives of sodium (R)-4-[(3R,5R,8R,9S,10S,12S,13R,14S,17R)-3,12-dihydroxy-10,13-dimethylhexadecahydro-1H-cyclopenta[a]phenanthren-17-yl] pentanoate (sodium deoxycholate) were synthesized by refluxing sodium deoxycholate with the corresponding trimethyl and triphenyltin (IV) chlorides in equimolar ratio in dry distilled toluene, refluxing for 7–8 h. Sodium chloride was removed by filtration and the soluble product was separated by evaporating toluene under vacuum using rotoevaporation. The product obtained was recrystallized in chloroform: n-hexane (1 : 2).

2.2.1 Synthesis of (R)-trimethylstannyl 4-[(3R,5R,8R,9S,10S,12S,13R,14S,17R)-3,12-dihydroxy-10,13-dimethylhexadecahydro-1H-cyclopenta[a]phenanthrene-17-yl] pentanoate [$\text{Ph}_3\text{SnC}_{24}\text{H}_{39}\text{O}_4$]_n

(Yield: 0.97 g, 73.4%). m.p. 118–119 °C. Elemental analysis, % Calculated (Found) for [$\text{C}_{27}\text{H}_{48}\text{O}_4\text{Sn}$]_n: C, 58.39 (57.68); H, 8.71 (8.56). FT-IR (cm^{-1}): 1564 $\nu(\text{COO})_{\text{asym}}$, 1407 $\nu(\text{COO})_{\text{sym}}$, $\Delta\nu = 157$, 557 $\nu(\text{Sn}-\text{C})$, 439 $\nu(\text{Sn}-\text{O})$, 615 (O–Sn–O). ^1H NMR (ppm): 1.27–2.05 (m, $\text{H}_{\text{cycloalkane}}$), 0.84–1.14 (m, H_2-H_5 , H_2O , H_{25}), 3.43 (bs, H_{16} , H_{24}), 0.37 (s, $\text{Sn}-\text{CH}_3$ [$^2J = 51.0$], $\theta = 107.6^\circ$).

^{13}C NMR (ppm): 177.9 (C-1), 12.3, 15.2, 17.3, 23.3, 24.4, 25.4, 25.4, 26.2, 26.9, 28.5, 30.3, 31.6, 33.2, 34.1, 35.5, 36.1, 40.6, 42.2, 46.4, 47.7, 48.0 (C_2-C_{14} , $\text{C}_{17}-\text{C}_{22}$, $\text{C}_{25}-\text{C}_{26}$), 73.3 (C_{15}), 72.2 (C_{23}), 10.2 ($\text{Sn}-\text{CH}_3$), 1J [$^{119}\text{Sn}-^{13}\text{C} = 352$, $\theta = 107.6^\circ$] ^{119}Sn (ppm): 340.

2.2.2. Synthesis of (R)-triphenylstannyl 4-[(3R,5R,8R,9S,10S,12S,13R,14S,17R)-3,12-dihydroxy-10,13-dimethylhexadecahydro-1H-cyclopenta[a]phenanthren-17-yl] pentanoate [$\text{Ph}_3\text{SnC}_{24}\text{H}_{39}\text{O}_4$]_n (2).

(Yield 1.49 g, 84.6%). m.p. 67–70 °C. Elemental analysis, % Calculated (Found) for [$\text{C}_{42}\text{H}_{54}\text{O}_4\text{Sn}$]_n: C, 68.02 (68.03); H, 7.34 (7.34). FT-IR (cm^{-1}): 1521 $\nu(\text{COO})_{\text{asym}}$, 1408 $\nu(\text{COO})_{\text{sym}}$, $\Delta\nu=113$, 282 $\nu(\text{Sn}-\text{C})$, 440 $\nu(\text{Sn}-\text{O})$, 610 (O–Sn–O). ^1H NMR (ppm): 1.26–2.03 (m, $\text{H}_{\text{cycloalkane}}$), 0.83–1.13 (m, H_2-H_5 , H_2O , H_{25}), 3.43 (bs, H_{16} , H_{24}), 7.77 (H_{ortho} , d), 7.42 (H_{meta} , dd), 7.48–7.56 (H_{para} , dd). ^{13}C NMR (ppm): 181.4 (C-1), 12.6, 15.4, 17.3, 23.1, 24.4, 25.1, 25.7, 26.1, 27.2, 28.6, 30.5, 31.7, 33.6, 34.1, 35.3, 36.0, 40.2, 42.1, 46.5, 47.4, 48.2 (C_2-C_{14} , $\text{C}_{17}-\text{C}_{22}$, $\text{C}_{25}-\text{C}_{26}$), 73.1 (C_{16}), 72.2 (C_{24}), 138.5 (C_{ipso}), 136.9 (C_{ortho}), 129.4 (C_{meta}), 131.3 (C_{para}). ^{119}Sn (ppm): 95.

3. RESULTS AND DISCUSSION

3.1 IR Analysis

Functional group investigation of coordination compounds 1 and 2 was carried out with FTIR analysis in the range 200 to 4000 cm^{-1} . $\nu(\text{COO})$, $\nu(\text{Sn}-\text{C})$, and $\nu(\text{Sn}-\text{O})$ are the peaks of interest in IR spectrum. The characteristic band at 1521–1571 cm^{-1} was attributed to $\nu_{\text{asym}}(\text{CO}_2)$, while vibrations appeared at 1404–1418 cm^{-1} are characteristic of $\nu_{\text{sym}}(\text{CO}_2)$; $\Delta\nu(\text{CO}_2)$ ($\Delta\nu = \nu_{\text{asym}} - \nu_{\text{sym}}$) below 150 cm^{-1} suggests a chelating mode of coordination, while difference between 150 and 250 cm^{-1} suggests a bridging coordination [13]. The $\Delta\nu$ for 1 and 2 clearly indicates bidentate bridging mode of coordination. FT-IR data suggests five-coordinate polymeric geometry in solid state.

3.2 Multinuclear NMR Analysis

^1H , ^{13}C , and ^{119}Sn NMR spectra of the compounds were recorded in CDCl_3 . However, due to complex structure, no fine pattern was observed. Owing to their multiplicity and intensity in a narrow range, multiplets and broad signals were

obtained. In **1**, methyl group protons gave a sharp singlet at 0.37 ppm with well-defined satellites due to Sn–¹H coupling in region expected for tetrahedral geometry [14], which shows dissociation of the polymeric structure in solution. For **2**, due to complex peak pattern, no couplings were observed. In ¹³C NMR spectra, new peaks for alkyl and aryl groups favor the formation of compounds. However, the environment of different carbons does not differ too much, and does not resonate at very different frequencies and appear in a narrow range. Methyl groups attached to Sn gave a peak in the upfield region. Coupling constant value of 352 for **1** suggests a tetrahedral geometry in solution [14], in agreement with ¹H NMR spectroscopic results. Carbons of butyl groups were assigned peak values by comparison to the literature [15]. Confirming solution state geometry, their ¹¹⁹Sn NMR spectra were taken in chloroform, where the chemical shift value gave information about geometry in solution. Increase in coordination number gives a large upfield shift. Only tetrahedral complexes are reported to show a positive chemical shift value and appear in the most downfield region. An increase in electron-releasing power of the alkyl group results in shifting of ¹¹⁹Sn value to higher field, as a consequence of increased shielding [16]. Appearance of single peaks in ¹¹⁹Sn NMR spectra supports the formation of one species and purity of the compounds. According to Holecek and co-workers, four, five, six, and seven coordination compounds give chemical shifts in the range of +200 to –60, –90 to –190, –210 to –400, and –440 to –540 ppm, respectively [17]. Compounds **1** and **2** gave resonances at a very downfield region at 340 and 310 ppm, respectively, which could be due to tetrahedral geometry. It is evident from the ¹H, ¹³C, and ¹¹⁹Sn NMR spectra that both compounds do not retain their five-coordinate geometry and exist as tetrahedra in solution.

3.3 Fluorescence Quenching

Fluorescence quenching of bovine and human serum albumin by the triorganotin(IV) complexes **1** and **2** was performed using fluorescence spectroscopy. The absorption spectra of three compounds were taken and overlapped with the fluorescence spectra of BSA and HSA to figure out their quenching ability. The spectral overlap of both compounds is shown in Figures (1 -9) The fluorescence spectra of albumin proteins in the absence and presence of increasing concentrations of compounds were recorded at two different temperatures, 293.15 K and 310.15 K. Fluorescence of BSA and HSA was quenched with the rise of temperature. These quenching experiments are essential to describe the fate of organotin compounds in the body. It has already been reported that organotin compounds could bind to HSA and then be transported after being imported into the bloodstream and translocated into the organs in the human body [11]. Quenching constants at two different temperatures were calculated, and a mechanism is proposed.

Generally, two different types of quenching, static and dynamic, describe the mechanism of binding the quencher with biomolecules in solution, *g* [18]. Static quenching results from a ground state complex formation between albumin protein and quencher, while dynamic quenching is due to the collision or diffusion of quencher and biomolecule [19]. If dynamic quenching is assumed to be the possible route of binding, then according to the Stern Volmer equation,

$$(F^0)/F = 1 + K_q\tau_0[Q] + K_{sv} [Q]$$

Where F^0 and F are the fluorescence intensities of BSA in the absence and presence of complexes, respectively, τ_0 is the average fluorescence lifetime without complexes. The binding constants were calculated by following expression.

The Stern Volmer plot for complexes sometimes shows deviations from linearity and positive or negative deviations. A downward curvature (negative deviation) suggests that static quenching occurs in the system. In such cases, the system follows a modified Stern Volmer equation which takes the form.

$$\frac{F^0}{F^0 - F} = 1 + \frac{1}{f_a K_a [Q]} + \frac{1}{f_a}$$

Where F^0 and F are the fluorescence intensities in the absence and presence of quenchers. $[Q]$ is the quencher concentration; K_a is the Stern Volmer quenching constant, and f_a is the intensity of accessible fraction in the presence of a quencher [20]. A positive deviation (curvature towards Y-axis) suggests the presence of both types of quenching mechanisms by the same fluorophore [21,22]. Eftink and Ghiron [23] reported that an upward curvature in the Stern Volmer plot directs an additional static quenching taking place near the subdomain(s) where tryptophan residues are residing [22].

A negative deviation from linearity suggests a ground state complex formation thus static quenching is favored. Both Stern Volmer and modified Stern Volmer equations were used to evaluate quenching. The effect of the temperature is useful parameter in deciding the mechanism of quenching. In case of static quenching, an increase in temperature destabilizes the complex formed and thus the quenching constant decreases [20].

The quenching constants in all cases are calculated by using modified Stern Volmer equation and are then collected in Tables 1-4

The results obtained revealed that the fluorescence of BSA was appreciably quenched by both compounds. However, only a slight quenching of fluorescence of HSA was observed. The observed behavior is certainly a consequence of less tryptophane content in HSA than in BSA. The quenching constant calculated from a modified Stern Volmer equation, revealed that quenching is directly related to the increase in the temperature which stabilizes the excited state complex and results in a dynamic or collisional quenching.

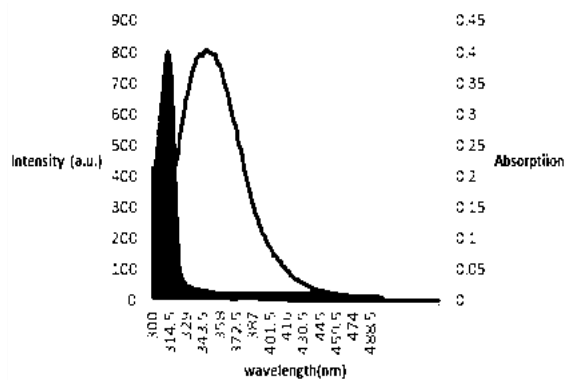


Figure 1: Spectral overlap of absorption spectrum of complex **1** with fluorescence spectrum of BSA

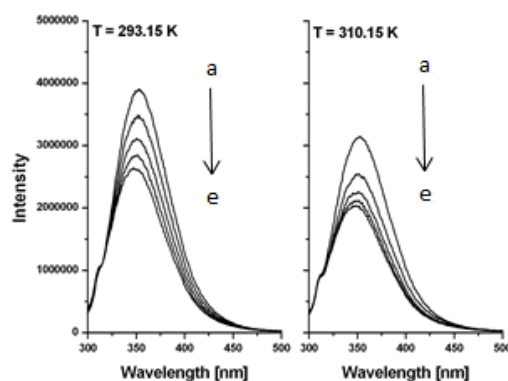


Figure 2: Fluorescence spectrum of 10 μM BSA in the absence (a) and in the presence of 1.66 μM (b), 3.34 μM (c), 4.99 μM (d), and 6.64 μM (e) of complex **1**.

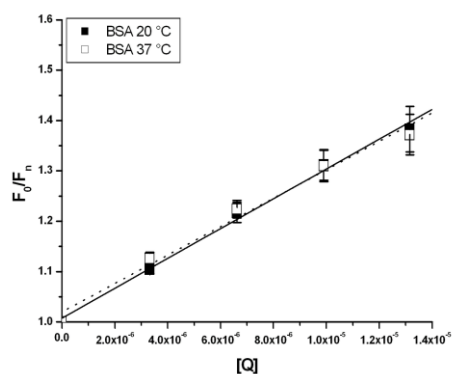


Figure 3: Stern Volmer plots for BSA with complex **1** for the calculation of quenching constants at 293 K and 310 K.

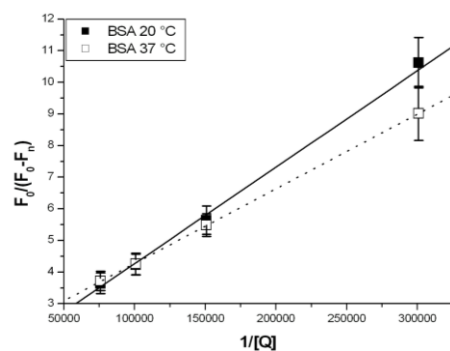


Figure 4: Modified Stern Volmer plots for BSA with complex **1** for the calculation of quenching constants at 293 K and 310 K

Table 1: Calculation of Quenching constants for BSA with complex **1** at 293.15K and 310.15K

Temperature	Stern-Volmer quenching constant of the accessible fraction in BSA		
	f_a^{-1}	$(f_a K_a)^{-1}$	K_a
293 K	1.21	3.04×10^{-5}	$3.9 \times 10^4 \text{ M}^{-1}$
310 K	1.9	2.3×10^{-5}	$8.0 \times 10^4 \text{ M}^{-1}$

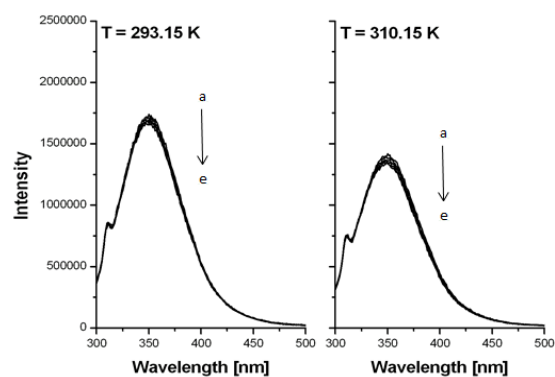


Figure 5: Fluorescence spectrum of 10 μM HSA in the absence (a) and in the presence of 1.66 μM (b), 3.34 μM (c), 4.99 μM (d) and 6.64 μM (e) of complex **1** at 293 K and 310 K

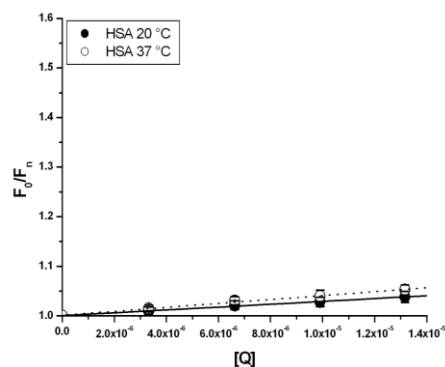


Figure 6: Stern Volmer plots for HSA with complex **1** for the calculation of quenching constants at 293 K and 310 K

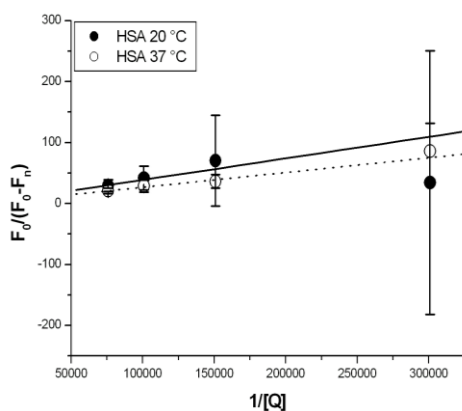


Figure 7: Modified Stern Volmer plots for HSA with complex **1** for calculation of quenching constants at 293.15 K and 310 K

Table 2: Calculation of Quenching constants for HSA with complex **1** at 293.15K and 310.15K

Temperature	Stern-Volmer quenching constant of the accessible fraction in HSA		
	f_a^{-1}	$(f_a K_a)^{-1}$	K_a
293 K	3.51	35.2×10^{-5}	$9.9 \times 10^3 \text{ M}^{-1}$
310 K	2.47	24.2×10^{-5}	$1.02 \times 10^4 \text{ M}^{-1}$

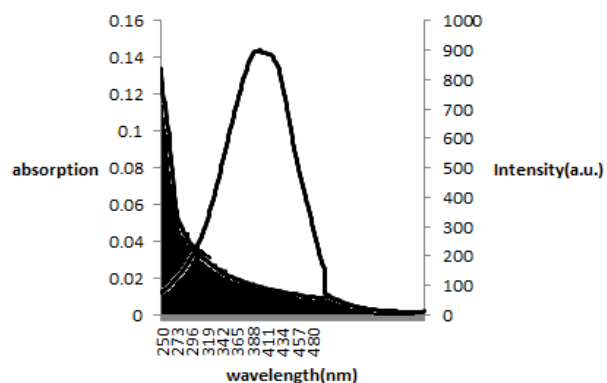


Figure 8: Spectral overlap of absorption spectrum of complex **2** with the fluorescence spectrum of BSA

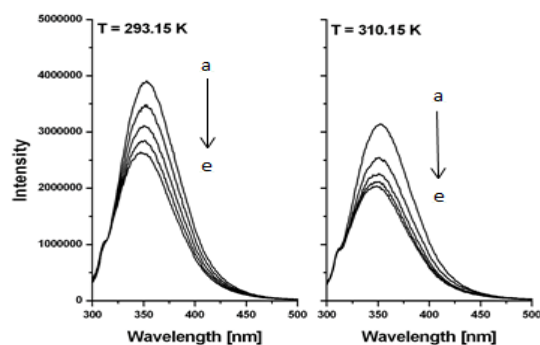


Figure 9: Fluorescence spectrum of 10 μM BSA in the absence (a) and in the presence of 1.66 μM (b), 3.34 μM (c), 4.99 μM (d), and 6.64 μM (e) of complex **2** at 293 K and 310 K

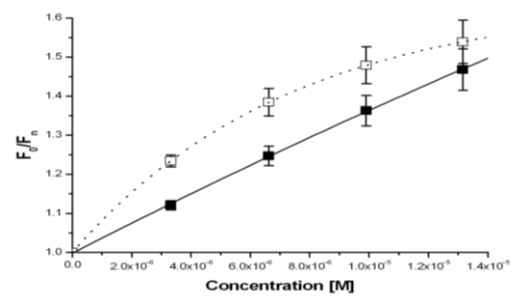


Figure 10: Stern Volmer plots for BSA with complex **2** for calculation of quenching constants at 293 K and 310 K

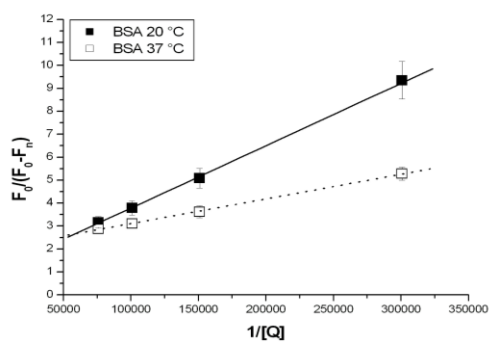


Figure 11: Modified Stern Volmer plots for BSA with complex **2** for calculation of quenching constants at 293.15 K and 310 K

Table 3: Calculation of Quenching constants for BSA with complex **2** at 293.15K and 310.15K

Temperature	Stern-Volmer quenching constant of the accessible fraction in BSA		
	f_a^{-1}	$(f_a K_a)^{-1}$	K_a
293.15 K	1.06	2.71×10^{-5}	$3.9 \times 10^4 \text{ M}^{-1}$
310.15 K	2.03	1.07×10^{-5}	$1.8 \times 10^5 \text{ M}^{-1}$

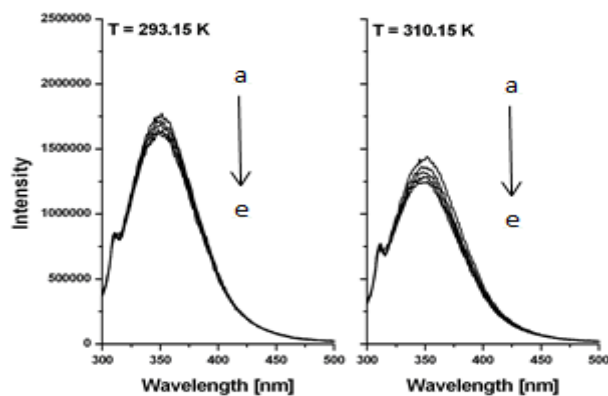


Figure 12: Fluorescence spectrum of 10 μM HSA in the absence (a) and in the presence of 1.66 μM (b), 3.34 μM (c), 4.99 μM (d), and 6.64 μM (e) of complex **2** at 293.15 K and 310 K

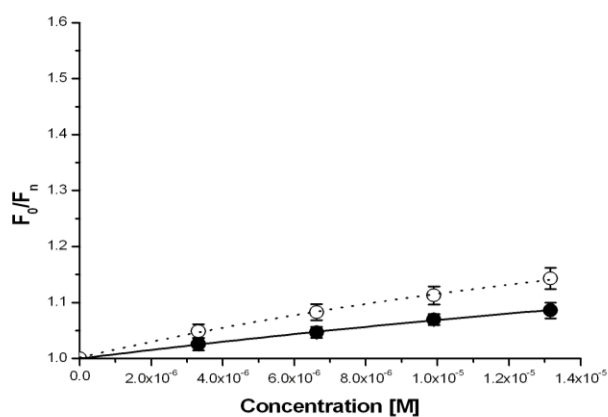


Figure 13: Stern Volmer plots for HSA with complex **2** for calculation of quenching constants at 293.15 K and 310 K

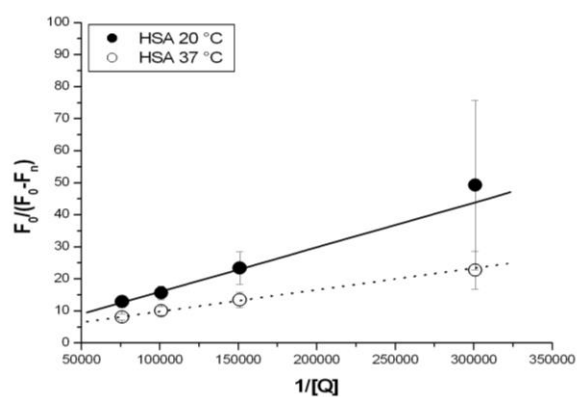


Figure 14: Modified Stern Volmer plots for HSA with complex **2** for calculation of quenching constants at 293.15 K and 310 K

Table 4: Calculation of Quenching constants for HSA with complex **2** at 293.15K and 310.15K

Temperature	Stern-Volmer quenching constant of the accessible fraction in HSA		
	f_a^{-1}	$(f_a K_a)^{-1}$	K_a
293.15 K	2.05	13.91×10^{-5}	$1.4 \times 10^4 \text{ M}^{-1}$
310.15 K	3.06	6.76×10^{-5}	$4.5 \times 10^4 \text{ M}^{-1}$

3.4 Synchronous Fluorescence

Synchronous spectroscopy is used primarily to obtain information about the composition of a complex mixture, where excitation and emission monochromators are scanned synchronously with a fixed wavelength between them ($\Delta\lambda$). The spectrum obtained by synchronous scanning varies with the wavelength span $\Delta\lambda$ [23]. Bovine and human serum albumin proteins are rich in their amino acid profile. Three critical structural units are responsible for the intrinsic fluorescence of these proteins, i.e., tryptophane, tyrosine, and phenylalanine. Tryptophane contributes significantly, while tyrosine and phenylalanine contribute negligibly in synchronous fluorescence spectroscopy. The distinction of the difference between the excitation wavelength and the emission wavelength ($\Delta\lambda$) reflects the spectra of distinct chromophores; with $\Delta\lambda$ of 60 nm, the synchronous fluorescence of BSA is characteristic of tryptophan residues and with $\Delta\lambda$ of 15 nm. It is characteristic of tyrosine [23].

Figure 15 shows, the synchronous fluorescence spectra of BSA upon addition of the increasing concentration of compound **1** from 0-12 μM , the quenching of the fluorescence intensity of tryptophan residues is stronger than that of the tyrosine residues, suggesting that the tryptophan residues contribute greatly to the quenching of intrinsic fluorescence.

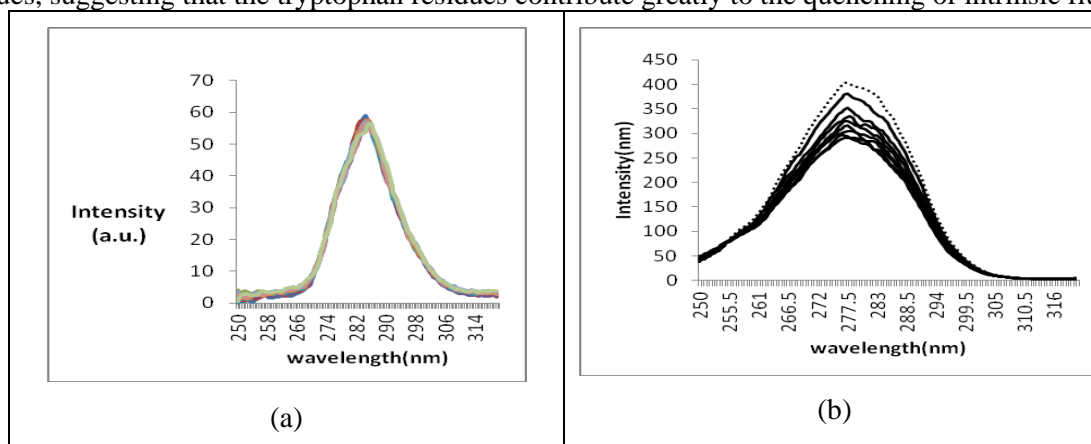


Figure 15: Synchronous fluorescence spectrum of BSA in the absence (dotted line) and presence of increasing concentration (solid lines falling downward) of compound **1** at $\Delta\lambda = 15 \text{ nm}$ (a) and $\Delta\lambda=60 \text{ nm}$ (b)

4. CONCLUSION

Interaction studies of trimethyl and triphenyltin(IV) deoxycholate complexes with bovine and human serum showed that both the compounds bind with BSA and HSA through dynamic quenching pathway at two different temperatures. Fluorescence quenching is appreciably due to the tryptophan residues of albumin proteins.

5. References

1. X. Meng, M.L. Leyva, M. Jenny, I. Gross, S. Benosman, B. Fricker, S. Harlepp, P. Hebraud, A. Boos, P. Wlosik, P. Bischoff, C. Sirlin, M. Pfeffer, J. Loeffler, and C. Gaidon, *Cancer Res.* 69(13): 5458-5466, (2009)
2. G. Gasser, I. Ott, and N. M. Nolte, *J. Med. Chem.* 54 (1): 3–25, (2011)
3. A. M. Graisa, A. A. Husain, M. H. Al-Mashhadani, D. S. Ahmed, H. Adil, E. Yousif, *Serambi Eng.* 1, 2631 – 2638, (2022)
4. S. N. S. Annuar, N. F. Kamaludin, N. Awang, K. M. Chan, *Front. Chem.* 9, 599-657 (2021)
5. T. Topalá1, A. Bodoki1, L. Oprean, and R. Oprean, *Clujul Med.* 87(4): 215-219, (2014)
6. S. Tabassum, R. A. Khan, F. Arjmand, S. Sen, J.J. Kayal, A. Juvekar, and S. M. Zingde, *J. Organomet. Chem.* 696(8): 1600-1608, (2011)
7. M. Nath, S. Pokharia, and R. Yadav, *Coord. Chem. Rev.* 215(1): 99-149, (2001)
8. L. Nagy, H. Mehner, A. Christy, E. Sletten, F. Edelmann, and Q. Andersen, *J. Radioanal. Nucl. Chem.* 227(1): 89-98, (1998)
9. M. Nath, S. Pokharia, X. Song, G. Eng, M. Gielen, M. Kemmer, M. Biesemans, R. Willem, and D. D. Vos, *Appl. Organometal. Chem.* 17: 305-314, (2003)
10. M. N. Xanthopoulou, S. K. Hadjikakou, N. Hadjiliadis, E. R. Milaeva, J. A. Gracheva, V. Y. Tyurin, N. Kourkoumelis, K. C. Christoforidis, A. K. Metsios, S. Karkabounas, and K. Charalabopoulos, *Eur. J. Med. Chem.* 43(2): 327-335, (2008)
11. J. Sun, B. He, Q. Liu, T. Ruan, and G. Jiang, *Talanta*, 93: 239-244, (2012)
12. F. Shaheen, S. Ali, S. Rosario, and N. A. Shah, *J. Coord. Chem.* 67(10): 851-186, (2014)
13. G. Deacon, R. Phillips, *Coord. Chem. Rev.* 33: 227-250, (1980)
14. T.P. Lockhart, W.F. Manders, E.M. Holt, *J. Am. Chem. Soc.* 108(21): 6611-6616, (1986)
15. C.C. Camacho, I.R. Oviedo, M.A.P. Sandoval, J. Cárdenas, A. Toscano, M. Gielen, L.B. Sosa, F.S. Bártéz, I.G. Mora, *Appl. Organomet. Chem.* 22(3): 171-176, (2008)
16. S. Shahzadi, S. Ali, K. Shahid, M. Yousaf, S.K. Sharma, K. Qanungo, *J. Chin. Chem. Soc.* 57, 659-670, (2010)
17. J. Holeček, M. Nádvorník, K. Handlíř, A. Lyčka, *J. Organomet. Chem.* 315(3): 299-308, (1986)
18. J. R. Lakowicz ; Principles of Fluorescence Spectroscopy, Boston, M.A., *springer*, US, pp.27-61, (2006).
19. J. Wang, D. Wang, D. Moses, and A. J. Heeger, *J. Appl. Poly. Sci.* 82(10): 2553-2557, (2001)
20. J. R. Albani; Structure and Dynamics of Macromolecules, Absorption and Fluorescence Studies, *Elsevier*, p. 167, (2011).
21. R. S. Kumar, P. Paul, A. Riyasdeen, G. Wagnieres, H. van den Bergh, M. A. Akbarsha, and S. Arunachalam, *Colloids Surf. B: Biointerfaces.* 86(1): 35-44, (2011)
22. M. R. Eftink, and C. A. Ghiron, *Anal. Biochem.* 114(2): 199-227, (1981)
23. R. S. Kumar, H. van den Bergh, and G. Wagnières, *J. Sol. Chem.* 41(2): 294-306, (2012)

Received: 12th August 2022

Accepted: 21th November 2022